LS Note 280

Benchmark and Comparisons of FEL Simulation Programs TDA3D and GENESIS

Y.-C. Chae, S. V. Milton
Argonne National Laboratory
Advanced Photon Source
9700 South Cass Avenue, Argonne, IL 60439

June 30, 1999

I. Introduction

A low-energy undulator test line (LEUTL) is under construction at the Advanced Photon Source (APS). This line will initially be used to demonstrate a free-electron laser (FEL) based on the self-amplified spontaneous-emission (SASE) process. The FEL simulation programs, TDA3D[1,2,3] and GENESIS[4], together with several other codes have been used for the LEUTL project. In order to increase the confidence on the simulation results, we attempted to benchmark two programs TDA3D and GENESIS. The results are reported here.

The programs TDA3D and GENESIS solve the paraxial FEL equations with the approximation that the amplitude of the radiation field is slowly varying;

$$\frac{d\gamma}{dz} = -k_s \frac{a_s a_w f_B}{\gamma} \sin(\theta + \phi_s)\,, \tag{1}$$

$$\frac{d\theta}{dz} = k_w - k_s \frac{1 + p_\perp^2 + a_w^2 + a_s^2 - 2a_s a_w f_B \cos(\theta + \phi_s)}{2\gamma^2}, \tag{2}$$

$$\frac{dp_\perp}{dz} = -\frac{1}{2\gamma}\frac{\partial a_w^2}{\partial r_\perp} \mp \gamma G_Q (x\hat{e}_x - y\hat{e}_y), \tag{3}$$

$$\frac{dr_\perp}{dz} = \frac{p_\perp}{\gamma}, \tag{4}$$

$$\left[2ik_s \frac{\partial}{\partial z} + \nabla_\perp^2\right] a_s e^{i\phi_s} = -\frac{eZ_0 I f_B}{mc^2}\left\langle \frac{a_w e^{-i\theta}}{\gamma}\right\rangle, \tag{5}$$

where

λ_w = undulator period,

k_w = $2\pi/\lambda_w$,

B_w	=	rms/peak magnetic field of a planar/helical undulator,
a_w	=	$\frac{eB_w}{mck_w}$, normalized undulator vector potential,
f_B	=	$[J_0(b)-J_1(b)]$, $b=a_w^2/(1+a_w^2)$, for a planar undulator, and 1 for a helical undulator,
G_Q	=	$B'/(B\rho)$, external focusing by quadrupole,
ω_s	=	angular frequency of the radiation field,
λ_s	=	wavelength of the radiation field,
k_s	=	$2\pi/\lambda_s$,
E_s	=	rms/peak electric field of the radiation from a planar/helical undulator,
a_s	=	$\frac{eE_s/c}{mck_s}$, normalized radiation vector potential,
ϕ_s	=	the phase of radiation vector potential,
γ	=	the particle energy in the unit of mc^2,
θ	=	$(k_s+k_w)z-w_st$, the particle phase,
$p_\perp$	=	the transverse canonical momentum in the unit of mc,
$r_\perp$	=	the transverse particle coordinate,
Z_0	=	$\mu_0 c$, impedance of free space,
I	=	beam current,
$\langle\cdots\rangle$	=	$\frac{1}{N}\sum_{j=1}^{N}(\cdots\cdots)$, average over *N* particles.

The numerical algorithms used in TDA3D and GENSIS that solve these equations are similar to each other. Both programs integrate a system of $6N_p$ particle equations, Eq. (1)-(4), in the x-y-z coordinate system. Major differences lie in solving the field equation, Eq. (5). TDA3D solves the equation in the cylindrical coordinate system. For a given azimuthal mode m, a system of $2(2m+1)N_r$ field equations are solved for the values at N_r radial grids. Thus the fundamental mode of a laser beam, TEM_{00} mode, can be well approximated with the single azimuthal mode m=0. Three-dimensional effects can be included by adding a few azimuthal modes up to m=4. GENESIS solves a system of equations for radiation field directly in the x-y-z coordinate system using the *alternating direction implicit (ADI)* method.

In our study we ran TDA3D solely in the m=0 axially symmetric radiation mode. By so doing we benchmark TDA3D as a 2-D code, while GENESIS is explicitly a 3-D code in the treatment of radiation field. Both programs, however, treat the electron dynamics three-dimensionally.

We will compare the amplification of input power along the undulator with the same or equivalent input parameters. The output of the two programs will then be put side-by-side. Input parameters were drawn from those expected for the LEUTL FEL and are shown in Table 1.

Table 1 Nominal Parameters Used in LEUTL FEL Simulation

Energy	E	220	MeV
Energy Spread	$\Delta E/E$	0.1	%
Normalized Emittance	ε_n	5.0	mm-mrad
Peak Current	I_p	150	Amp
Undulator Period	λ_w	3.3	cm
Undulator Parameter (Peak)	K	3.1	
Undulator Parameter (rms)	a_w	2.192	
Matched Beta-Function	β_0	1.46	m
Resonance Wavelength	λ_r	516.751	nm
Optimum Wavelength	λ_{opt}	517.785	nm
Number of Particle (GENESIS)	N_p	4086	
Number of Particle (TDA3D)	N_p	8196	
Input Power	P_{in}	1, 10	W
Rayleigh Length	Z_R	0.8	m
Position of Beam Waist	Z_w	0	m

In order to further benchmark GENESIS and TDA3D, we compare the simulation results with those of the theory. One readily available quantity for comparison is the gain length in the exponential gain regime.

Free-electron-laser gain including all the effects of energy spread, emittance, focusing of the electron beam, and the diffraction and guiding of the radiation has been calculated by several authors for the exponential gain regime before the saturation. Yu, Krinsky and Gluckstern[5] were the first to derive and solve such a dispersion relation by a variational method. They showed that the growth rate can be expressed as a function of a few dimensionless quantities. The growth rate obtained by numerically solving the dispersion relation was compared with the simulation results and found to be in good agreement. In their comparison the FEL simulation programs FELEX and FRED had been used.

Later Chin, Kim, and Xie[6] derived and solved a similar dispersion relation by using the systematic mode-expansion method. The growth rate from this study was also shown to be in the same scaled form as Yu et al.,[5] and can be written as

$$\frac{\mathrm{Re}(q)}{k_w D} = F\left(2k_r\varepsilon_x, \frac{\sigma_\gamma}{D}, \frac{k_\beta}{k_w D}, \frac{k_s - k_r}{k_r D}\right), \qquad (6)$$

where Re(q) is the growth rate, $k_r = 2k_w\gamma^2/(1+a_w^2)$ is the resonant radiation wave number corresponding to the energy γ. The quantity D is the scaling parameter defined by

$$D = \sqrt{\frac{8}{\gamma}\frac{a_w^2}{1+a_w^2}\frac{I}{I_A}}\, f_B, \qquad (7)$$

where I is the beam current, and $I_A = ec/r_e \sim 17.05$ kA is the Alfven current. They compared the growth rate obtained by solving Eq. (6) in the form of a dispersion relation with the

simulation results from TDA3D. The comparison showed very good agreement over a wide range of parameters.

The successful comparison of the theory with the simulations was achieved for a circular electron-beam matched to the constant focusing channel. Also the wavelength was chosen to satisfy the relation

$$\frac{k-k_r}{k_r D} = -3\left(\frac{k_\beta}{k_w D}\right)k_r \varepsilon\,, \tag{8}$$

which was found to yield near-maximum growth.[5]

Solving the dispersion relation may be straightforward, but it is still a numerically involved process. A much simpler algorithm was developed by Xie,[7] which expresses the 3-D gain length as the explicit functions of scaled parameters. The expression, obtained by fitting to the numerical solution of dispersion relation in the scaled form of Eq. (6), is given by

$$\frac{L_{1d}}{L_g} = \frac{1}{1+\eta}\,, \tag{9}$$

where L_{1d} is 1-D gain length, L_g is 3-D gain length, and

$$\begin{aligned}\eta = {} & a_1\eta_d^{a_2} + a_3\eta_\varepsilon^{a_4} + a_5\eta_\gamma^{a_6} \\ & + a_7\eta_\varepsilon^{a_8}\eta_\gamma^{a_9} + a_{10}\eta_d^{a_{11}}\eta_\gamma^{a_{12}} + a_{13}\eta_d^{a_{14}}\eta_\varepsilon^{a_{15}} \\ & + a_{16}\eta_d^{a_{17}}\eta_\varepsilon^{a_{18}}\eta_\gamma^{a_{19}}\,.\end{aligned} \tag{10}$$

With the scaled parameters defined as

$$\eta_d = \frac{L_{1d}}{Z_R},\ \eta_\varepsilon = \left(\frac{L_{1d}}{\beta}\right)\left(\frac{4\pi\varepsilon}{\lambda}\right),\ \eta_\gamma = 4\pi\left(\frac{L_{1d}}{\lambda_w}\right)\left(\frac{\sigma_E}{E}\right), \tag{11}$$

where β is the matched beta-function, σ_E is the rms energy spread, Z_R is Rayleigh length defined as $Z_R = 4\pi\sigma_x^2/\lambda$, σ_x is rms transverse electron beam size, fitting parameters are found to be

a_1=0.45,	a_2=0.57,	a_3=0.55	a_4=1.6,	a_5=3.0,	a_6=2.0,
a_7=0.35,	a_8=2.9,	a_9=2.4,	a_{10}=51,	a_{11}=0.95	a_{12}=3.0,
a_{13}=5.4,	a_{14}=0.7,	a_{15}=1.9,	a_{16}=1140,	a_{17}=2.2,	a_{18}=2.9,
a_{19}=3.2.					

We will compare the gain length obtained by using Eq. (9) with the simulation results. Note that the above formula is valid for the de-tuning given by Eq. (8). As a reference for the parameters shown in Table 1, the optimum wavelength predicted by theory, Eq. (8), is $\Delta\lambda/\lambda=1.526\times10^{-3}$.

II. Benchmark Procedure

We describe the procedure used to find a set of simulation parameters that will be used for benchmarking the programs.

1. Find Optimum Wavelength

As the first step we try to find the optimum wavelength that will give the fastest growth in order to properly compare with theory later. The tuning range used in the GENESIS simulations was $\Delta\lambda/\lambda=\pm 5\times 10^{-3}$. Output power along the undulator for different wavelength are shown in Figure 1 on a semilog plot. This plot clearly shows the exponential gain regime in the middle of undulator. We could do an exponential fit to the output power as function of distance so that we can directly estimate the gain length, but previous experience showed that averaging the growth rate over chosen range resulted in a more reliable and accurate estimate of the gain length. Here the growth rate is defined as

$$g(z) = \frac{d\ln\left(p(z)/p(0)\right)}{dz} \quad , \qquad (12)$$

which is the inverse of gain length, $L_g(z)=1/g(z)$.

The growth rates for different wavelengths are shown in Figure 2. We chose the range where the growth rate is roughly constant between 6 m and 10 m, and then took an average over this region. The resultant de-tuning curve, gain length vs. wavelength, is shown in Figure 3. Note that the horizontal axis is the wavelength normalized by the resonance wavelength, which is

$$\lambda_r = \frac{\lambda_w}{2\gamma^2}\left(1+\frac{K^2}{2}\right) = 516.751 \text{ nm.}$$

We found that the minimum gain length (or maximum growth rate) can be achieved by de-tuning the wavelength to $\lambda=1.002\lambda_r$. The de-tuning curve for the saturation length is shown in Figure 4. Again the same wavelength resulted in the shortest saturation length consistent with the minimum gain length. We will call this the optimum wavelength. All following simulations were done at this optimum wavelength,
$\lambda_{opt} \equiv 1.002\lambda_r = 517.785 \text{ nm}$.

2. Convergence Test on Number of Simulation Particle

A set of runs were made to analyze the convergence properties of the simulation results as a function of the number of simulation particles for the beam of finite emittance and energy spread.

The test was done assuming a beam with the maximum energy spread considered in the benchmark, which is $\sigma_E / E = 0.2\%$. Each curve in Figure 5 represents the result for a different number of simulation particles, namely N_p=1024, 2048, 4096, 8192,

respectively, and shows that the calculation of growth rate converges at roughly 4096 particles.

3. Convergence Test on Rayleigh Range

In both GENESIS and TDA3D, the initial radiation profile is assumed to be a Gaussian TEM_{00} mode at z=0. We recall that the propagation in vacuum for this mode is governed by[1]

$$\begin{aligned} a_s(r,z)e^{i\phi_s(r,z)} &= \sqrt{\frac{2}{\pi}}a_{s0}\frac{w_0}{w(z)}e^{-r^2/w^2(z)}e^{i\phi_s(r,z)}, \\ w^2(z) &= w_0^2\left[1+\left(z-Z_w\right)^2/Z_R^2\right], \\ \phi_s(r,z) &= -\tan^{-1}\left[\left(z-Z_w\right)/Z_R\right]+\frac{k_s r^2}{2}\frac{z-Z_w}{\left(z-Z_w\right)^2+Z_R^2}, \end{aligned} \tag{13}$$

where w_0 is the minimum spot size, $Z_R = \pi w_0^2/\lambda_s$ is the Rayleigh length and Z_w is the position of the radiation waist. Since we can express the input power in terms of a_{s0} as

$$P_{in}(0) = \left(\frac{mc^2}{e}\right)^2 \frac{k_s^2 w_0^2}{Z_0} a_{s0}^2, \tag{14}$$

the initial profile at z=0 can be completely specified by four parameters, namely, the radiation wavelength, λ_s, the input power, P_{in}, the Rayleigh length (or the minimum spot size), Z_R, and the position of the beam waist, Z_w, as

$$a_s(r,0)e^{i\phi_s(r,0)} = \sqrt{\frac{2}{\pi}}a_{s0}\frac{w_0}{w(0)}e^{-Cr^2}, \text{ with } C = \frac{k_s/2}{Z_R - iZ_w}. \tag{15}$$

Assuming that the electron beam is matched at the entrance of the undulator, we set the position of the beam waist at the entrance, Z_w=0. Then the filling factor, the overlap between the electron and radiation beam, is determined by the Rayleigh length. For the parameters in Table 1, we find Z_R=0.42 m. However, our interests are in the interaction occurring in the exponential gain regime. The resultant gain length during exponential growth shouldn't be sensitive to the initial choice of the filling factor or Z_R.

The sensitivity of gain length on the choice of the Rayleigh length (or filling factor) is shown in Figure 6. In the early part of the undulator up to z=5 m, we find that a shorter Rayleigh length results in a smaller growth rate due to a larger diffraction loss. However, once well into the exponential gain regime, the GENESIS simulation shows that the growth rate does not depend on the initial condition of the radiation beam.

In the benchmark we used a Rayleigh length of 0.8 m. This allowed us to encompass the case of the segmented LEUTL FEL with an elliptical beam. Again this choice shouldn't change the outcome of gain length determination.

In the above we describe the procedures taken for deciding a few simulation parameters used in benchmarking the program GENESIS. We followed the same procedure for TDA3D. Here we found that the optimum wavelength from the TDA3D simulation is the

same as that found with GENESIS, namely $\lambda_{opt} \equiv 1.002\lambda_r = 517.785\ \mathrm{nm}$. A notable difference is that the TDA3D simulation required more simulation particles than GENESIS for an adequate description of the exponential gain regime. All TDA3D simulations were done with N_p=8192.

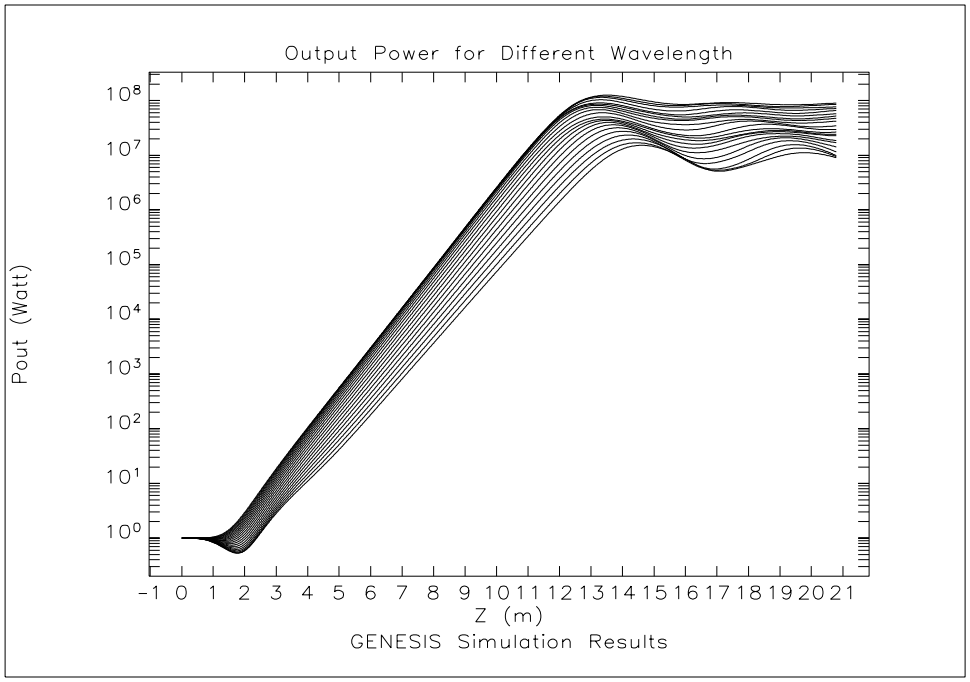

Figure 1: Power output along the undulator for different wavelengths.

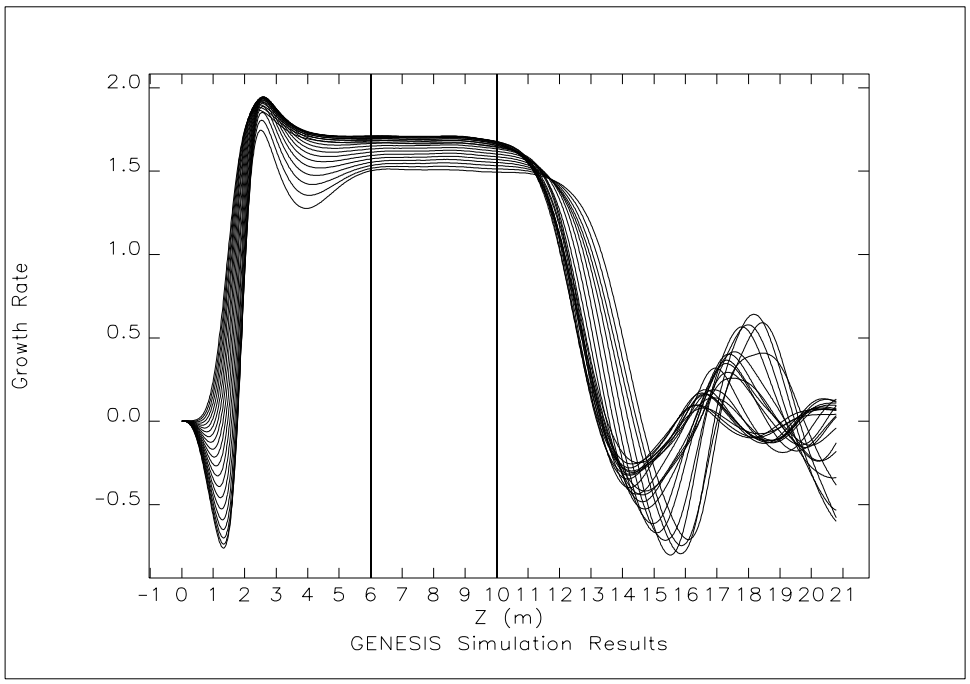

Figure 2: Growth rate along the undulator for different wavelengths.

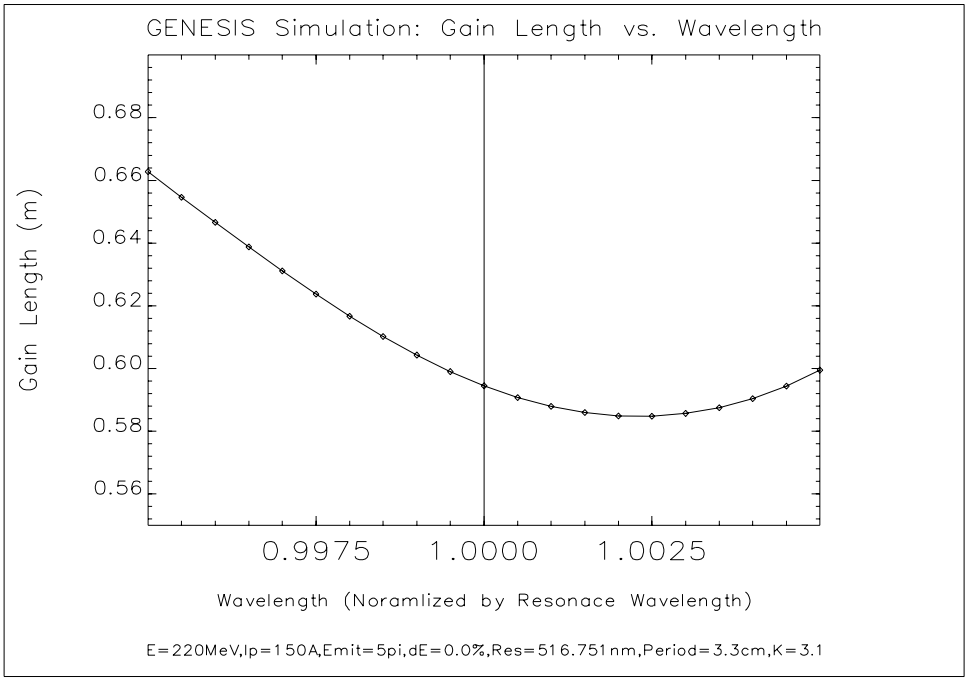

Figure 3: Gain length as function of wavelength.

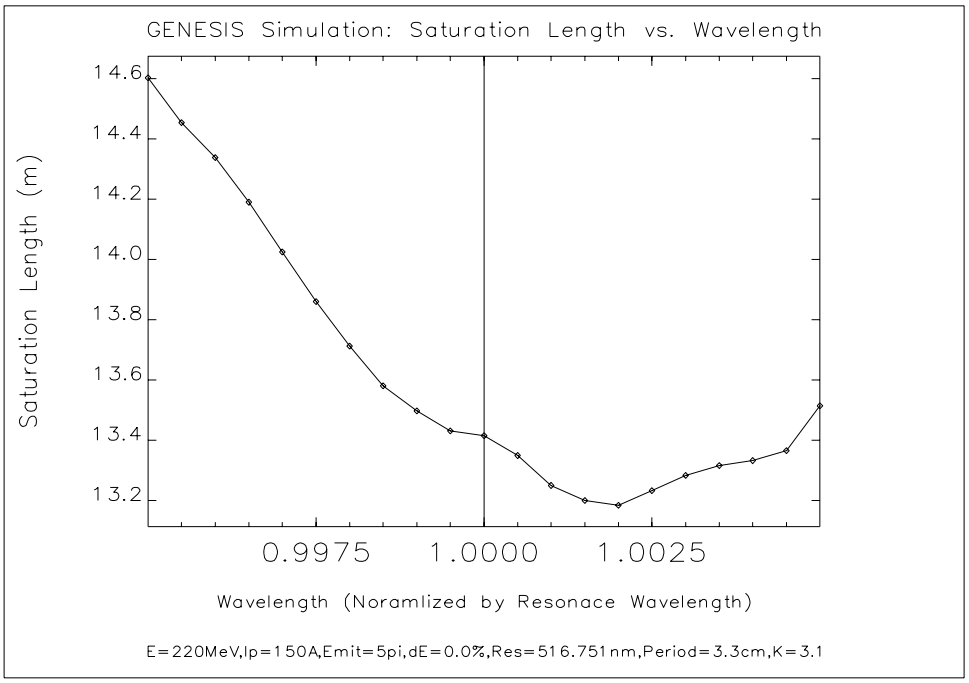

Figure 4: Saturation length as function of wavelength.

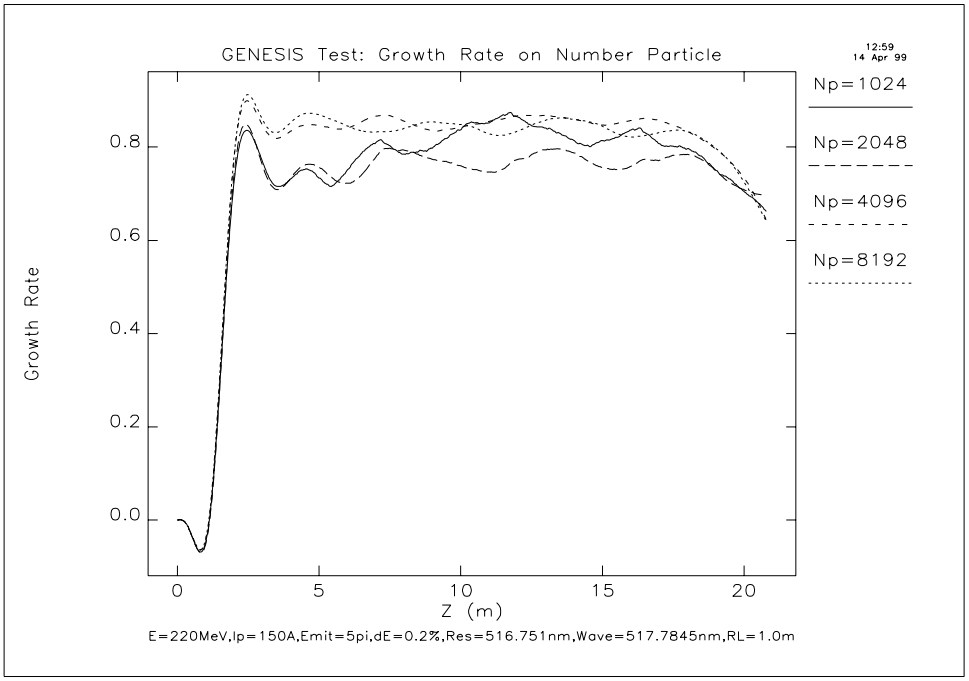

Figure 5: Growth rate as function of z for different values of the number of particles, Np.

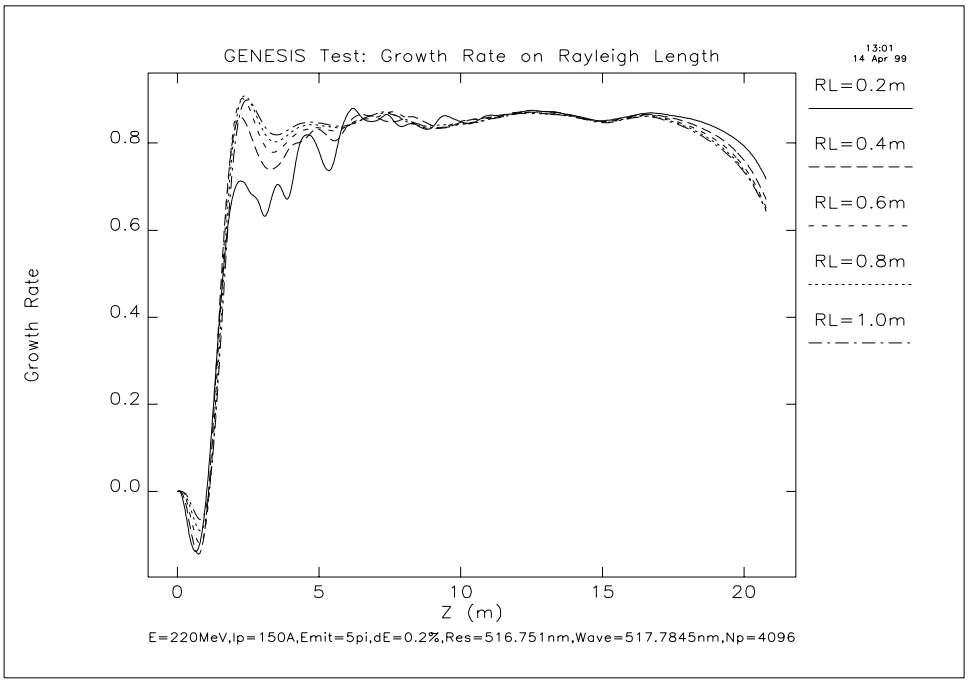

Figure 6: Growth rate simulation for different Rayleigh lengths.

III. Benchmark Results

In the real LEUTL FEL, several short undulator cells will be utilized. The empty space between the undulators will contain the focusing quadrupole and diagnostic devices. The undulator is planar with 70 periods and has a natural focusing in the non-wiggle plane only. Its strength is given by

$$G \equiv \frac{B'}{(B\rho)} = \frac{1}{2}\frac{B_0^2}{(B\rho)^2}, \qquad (16)$$

where B_0 is the peak undulator field. Note that, since $B_0 \approx 1\,\mathrm{T}$, the undulator focusing is strong for energies less than roughly 1 GeV. For LEUTL parameters we found that

$$B_0 = 1\,\mathrm{T},\ (B\rho) = 0.733\ \mathrm{T\ m}\ \text{for}\ E = 220\ \mathrm{MeV}\ \rightarrow\ G = 0.93\ \mathrm{m}^{-2}.$$

For comparison, the strongest quadrupole in the 7-GeV APS storage ring is Q4 whose strength is $G = 0.81\ \mathrm{m}^{-2}$. The focusing in the wiggle plane (the horizontal plane in LEUTL FEL) is achieved by the use of the external quadrupoles between undulator cells.

By placing the horizontally focusing quadrupole between the undulators, the LEUTL FEL consists of a periodic FOFO configuration in the horizontal direction and a FDFD lattice in the vertical plane. The lattice function of a periodic segment was calculated by the beam optics program MAD and is shown in Figure 7.

For the benchmark we consider three cases, (a) a long planar undulator with symmetric x-y focusing, (b) a long planar undulator with asymmetric x-y focusing, and (c) the segmented undulator case chosen for the LEUTL FEL as shown in Figure 7. For case (a) the linear theory is well developed so comparison between theory and simulation could be used to establish the validity of the simulation. For case (b) the theoretical result is in the form of formulation that needs to be further investigated. Here comparison with simulation could verify the theory. For case (c), there is no existing theory generalized to the LEUTL configuration; however, comparison of the results from the two different programs could be used to check one other.

1. Circular Beam, Matched to Symmetric Focusing Channel

Here we use a long planar undulator with equal focusing in both planes. The focusing strength is half that of the natural focusing of a planar undulator. This can be achieved by providing an external quadrupolar field along the undulator. We also match the electron beam to this focusing channel by proper choice for the initial phase ellipse of the electron beam. The resultant electron beam will be circular and have a radius that is constant along the undulator.

With this input beam we varied the other physical parameters, the peak current, emittance, or energy spread. Then we compared the results with theory. The gain length as functions of the peak current, emittance, and energy spread are shown in Figures 8,9, and 10, respectively. Recall that the resonant wavelength determined by the electron beam energy and undulator parameter is 516.751 nm, but the simulations were carried out

with an input wavelength of $\lambda \equiv 1.002\lambda_r = 517.785$ nm as shown in Table 1. Every case shows good agreements between the results of the two simulation program and the theoretical results obtained via Xie's algorithm. The primary difference is that the simulations show slightly larger gain length than predicted by Xie's algorithm.

More direct comparisons between the two programs were made. We show the amplifications of input radiation along the long undulator in Figure 11. In this log-plot we can hardly distinguish the two different outputs from one another. The saturation powers predicted by the phenomenological theory of Xie's work[7] and by the simulation are compared in Table 2. Again they agree very well.

Even though it is not shown here, both the theory and simulation results consistently have shown that the fundamental guided mode, namely the Gaussian TEM_{00} mode, dominates the FEL interaction in the exponential gain regime. The result is that the radiation output of the FEL is transversely coherent.[8] We believe that this is the reason for such good agreement between the 3-D simulation of GENESIS and the essentially 2-D simulation of TDA3D in which an axially symmetric m=0 mode is explicitly assumed.

Table 2: Saturation Power Predicted by Simulation Programs and Theory

Method	Saturation Power
TDA3D Simulation	73.20 MW
GENESIS Simulation	70.74 MW
Theory in reference [7]	72.80 MW

2. Elliptical Beam, Matched to Asymmetric Focusing Channel

So far the comparisons were made for the case of a round electron beam matched to the constant focusing channel. Since the ultimate objective of this study is to make sure that the simulation programs calculate all FEL output correctly for the realistic LEUTL configuration depicted in Figure 7, our next logical step was to benchmark the codes for the beam with an elliptical cross section.

The theoretical calculation of 3-D gain was generalized to the elliptical cross section in reference [6]. The results can be put into a form very similar to Eq. (6) as

$$\frac{\mathrm{Re}(q)}{k_w D} = F(2k_r\varepsilon_x, 2k_r\varepsilon_y, \frac{\sigma_\gamma}{D}, \frac{k_{\beta x}}{k_w D}, \frac{k_{\beta y}}{k_w D}, \frac{k-k_r}{k_r D}). \tag{17}$$

In particular, for a electron beam with Gaussian distribution given by

$$f_{0\perp}\left(r_x, r_y\right) = \frac{1}{(2\pi)^2 k_{\beta x}\sigma_x^2 k_{\beta y}\sigma_y^2}\exp\left[-\frac{r_x^2}{2\sigma_x^2} - \frac{r_y^2}{2\sigma_y^2}\right], \tag{18}$$

$$f_{0\parallel}(\gamma) = \frac{N}{\hat{\tau}}\frac{1}{\sqrt{2\pi}\sigma_\gamma\gamma_r}\exp\left[-\frac{(\gamma-\gamma_r)^2}{2\gamma_r^2\sigma_\gamma^2}\right], \tag{19}$$

the dispersion relation for the growth rate can be written in the scaled form[6]

$$1 = i\frac{\sqrt{\frac{k_{\beta x}}{k_w D}}\sqrt{\frac{k_{\beta y}}{k_w D}}}{4\pi\sqrt{2\pi}\sqrt{2k_r\varepsilon_x\sqrt{2k_r\varepsilon_y}}}\int_0^\infty\int_0^\infty\int_{-\infty}^\infty \frac{\exp\left[-\frac{s^2+u^2+v^2}{2}\right]ds\cdot udu\cdot vdv}{\left\{\frac{q}{k_W D} + 2i\frac{\sigma_\gamma}{D}s - \frac{i}{4}a\left[2k_r\varepsilon_x\frac{k_{\beta x}}{k_w D}u^2 + 2k_r\varepsilon_y\frac{k_{\beta y}}{k_w D}v^2\right]\right\}}$$
$$\times\int_{-\infty}^\infty\int_{-\infty}^\infty \frac{\exp\left[-\alpha^2-\beta^2\right]d\alpha\cdot d\beta}{\frac{q}{k_w D} + i\frac{k-k_r}{k_r D} + i\left[\frac{\alpha^2}{2k_r\varepsilon_x}\frac{k_{\beta x}}{k_w D} + \frac{\alpha^2}{2k_r\varepsilon_x}\frac{k_{\beta x}}{k_w D}\right]}. \tag{20}$$

The solution of the above dispersion relation is the growth rate of the fundamental mode, whose mode shape is in the same bi-Gaussian form of the electron beam Eq. (18). Assuming the fundamental mode dominates in the exponential gain regime as seen in the circular beam case, the solution of Eq. (20) will be a good approximate solution.

Solving Eq. (20) even for only the fundamental mode required a lengthy numerical integration. In fact, it sometimes took more time to solve Eq. (20) than to run TDA3D or GENESIS.

For comparison we chose electron beam parameters that are identical to those of a circular beam except that we varied the aspect ratio σ_x / σ_y while the cross-sectional area remained the same. The growth rates from three different methods are shown in Figure 12 as function of the aspect ratio. The values are normalized by the circular beam. Obviously it shows that the circular beam best amplifies the radiation.

Comparison between theory and GENESIS shows the anticipated behavior, that is, as the beam becomes more elliptic, 3-D effects become more important and the theory, which only considers the fundamental mode, begins to deviate from reality.

We find the good agreement between GENESIS and TDA3D up to the aspect ratio equal to 3.5. This is surprising, because in the TDA3D simulation only the Gaussian TEM_{00} mode was tracked and not the elliptic mode.

In this section we showed that the full 3-D simulation supports the theoretically calculated growth rate. Still many interesting questions remain to be investigated, for example, how to optimize the asymmetric focusing for beams with asymmetric emittances, what kind of mode shape to expect from an elliptic beam, etc.

3. Elliptical Beam, Matched to Periodic LEUTL Lattice

The beam matched to the periodic lattice of the LEUTL FEL will exhibit an envelope modulation as the beam size varies as $\sigma_{x,y} = \sqrt{\varepsilon_{x,y}\beta_{x,y}}$. In the case of the LEUTL, the β-function varies as shown in Figure 7. The maximum aspect ratio is about 1.5. This is relatively small so we expect that the LEUTL FEL operates in the regime where a 2-D simulation could provide reasonably accurate results.

We show the output power along the LEUTL FEL in Figure 13. Included in the simulation was the beam size modulation due to the varying β-function. The close agreement between TDA3D and GENESIS suggests that, for this case, the fundamental TEM_{00} mode still dominates as it does for the circular beam case, which implies that the average β-function is the important quantity to optimize. Regarding this statement, a detailed study will be reported separately, but we can convince ourselves by comparing the growth rates for the long and the segmented undulator cases.

The β-function in the long undulator is 1.46 m as shown in Table 1. The average β-function for the LEUTL lattice is about 1.6 m. The growth rates for two cases are shown in Figure 14. The average growth rate for the segmented lattice is slightly smaller than that for the long undulator, but they are very close to each other.

Another inspection of Figure 14 reveals that, since the undulator segments are short in the LEUTL FEL, it is difficult to define the exponential gain regime without ambiguity. Thus, the gain length is not a very good parameter for comparison. We suggest the saturation length/power as the comparison/optimization quantity in future simulation studies for the LEUTL FEL.

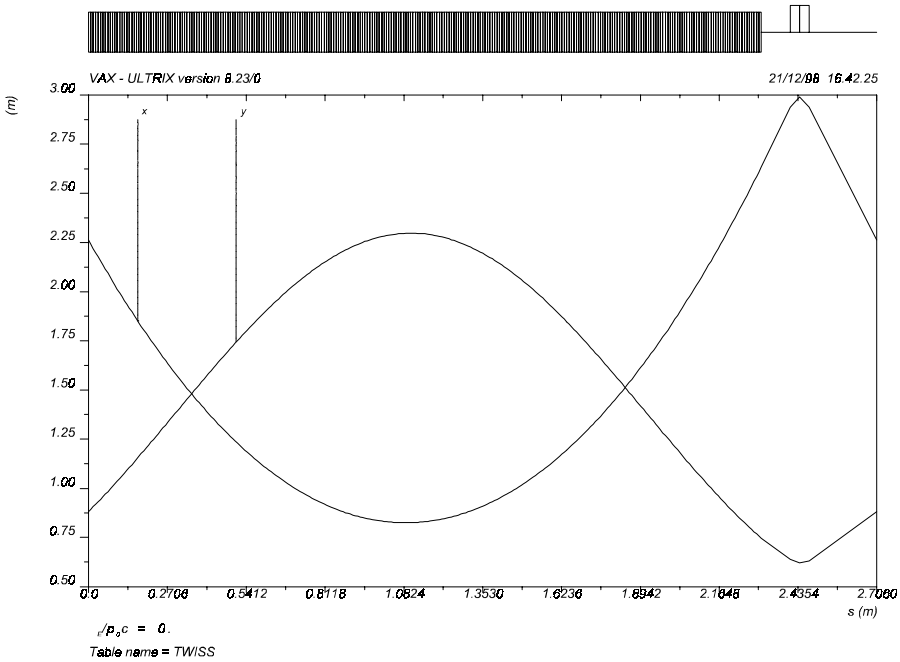

Figure 7: Lattice function of LEUTL FEL beam line.

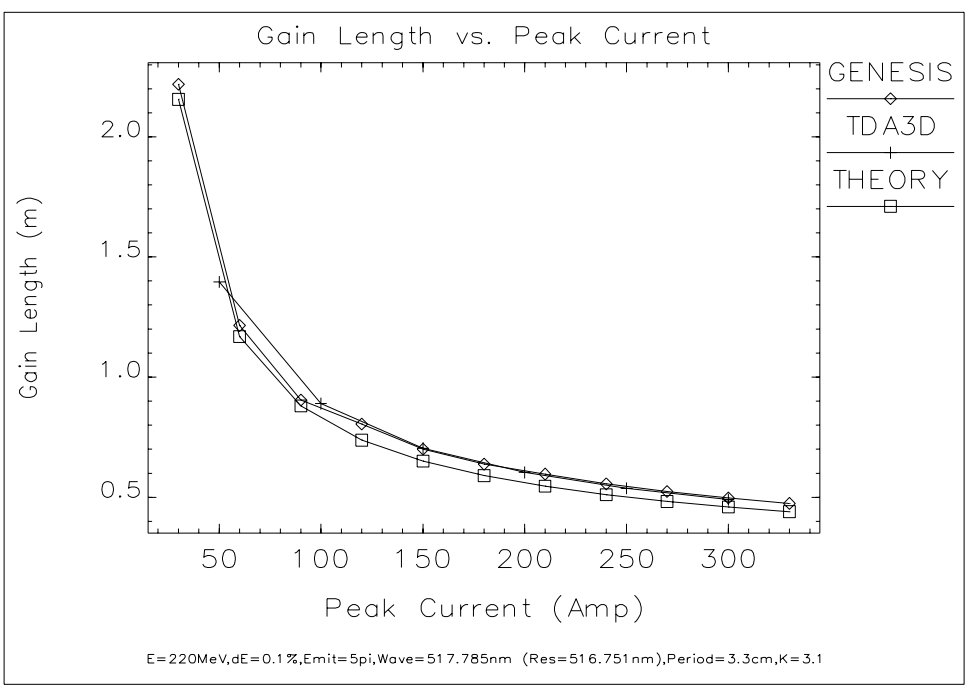

Figure 8: Gain length vs. peak current.

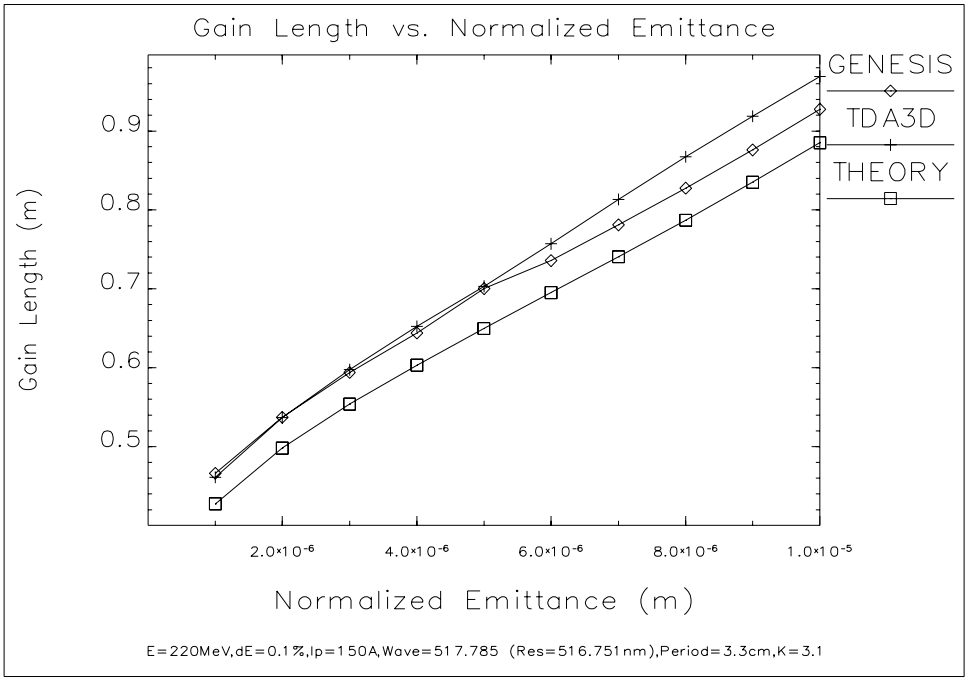

Figure 9: Gain length vs. emittance.

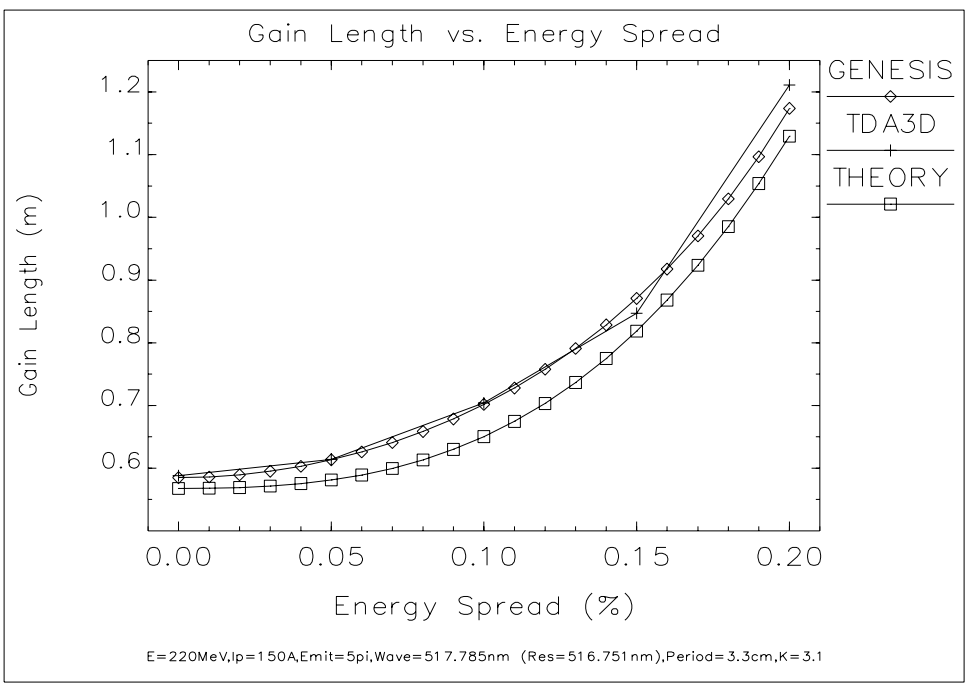

Figure 10: Gain length vs. energy spread.

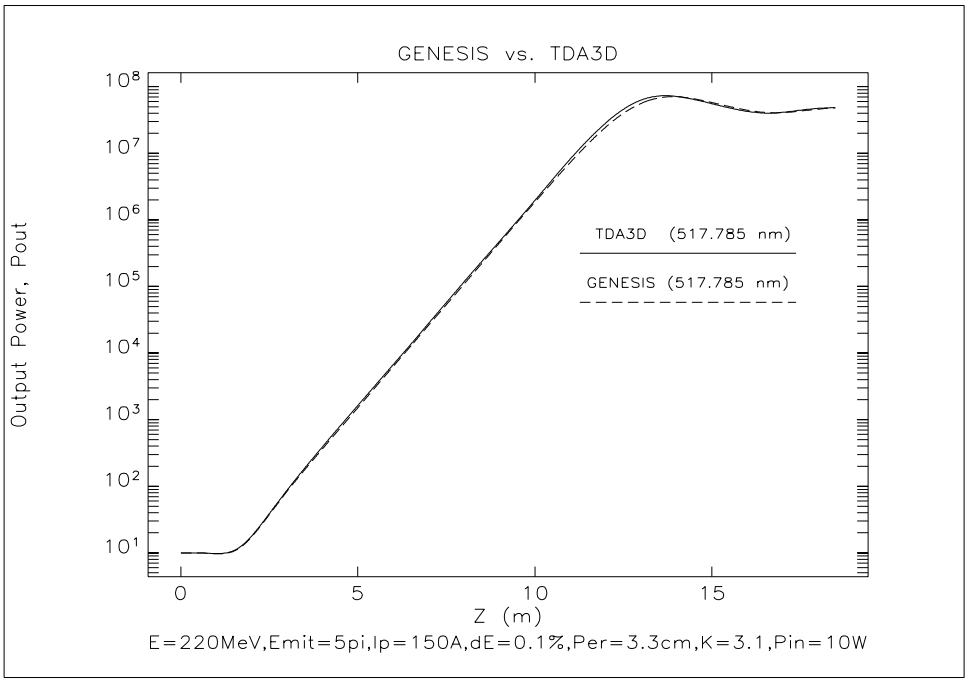

Figure 11: Input power amplification along the long undulator (solid line for TDA3D and dashed line for GENESIS).

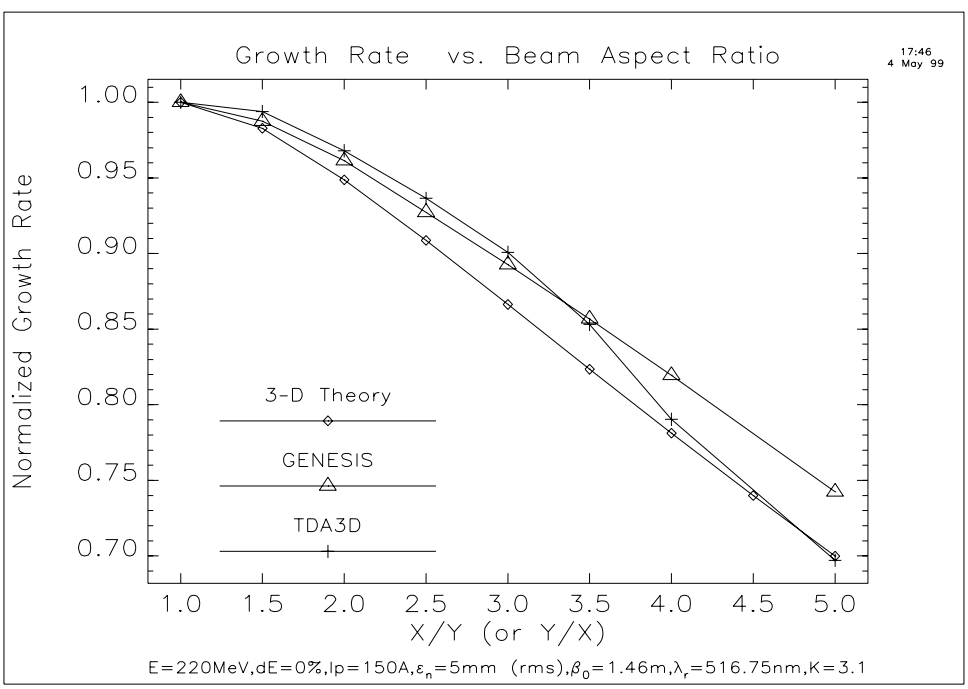

Figure 12: Growth rate as a function of beam aspect ratios.

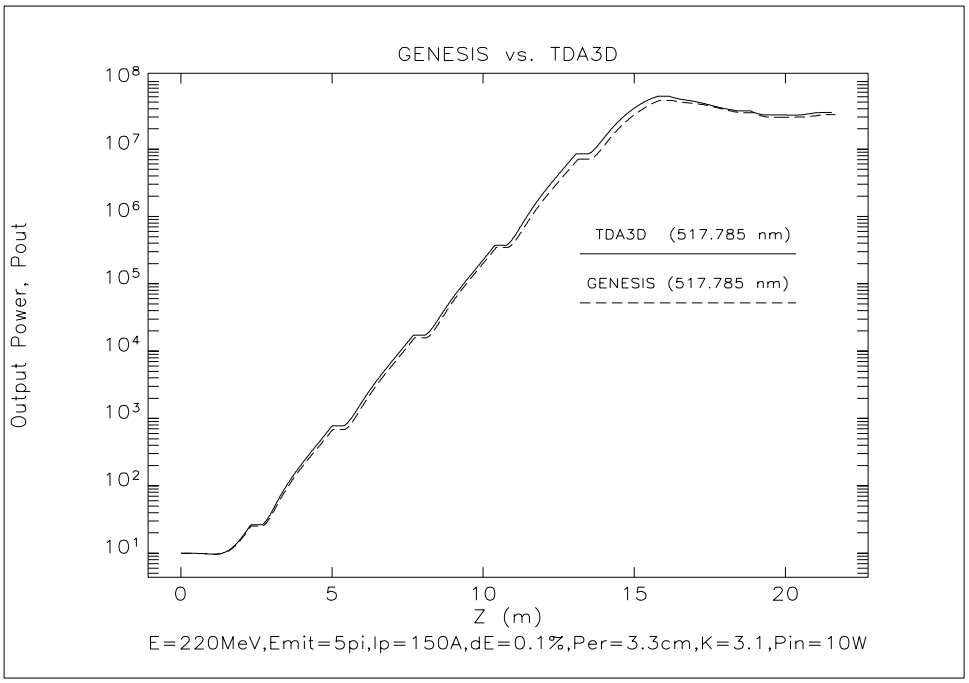

Figure 13: Comparison of output power along the LEUTL FEL.

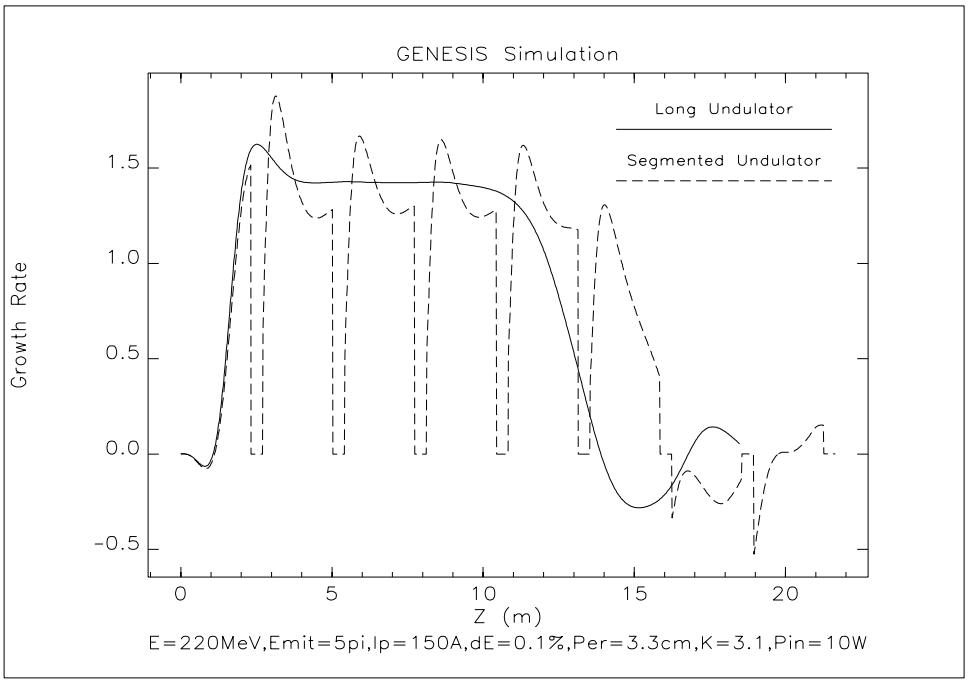

Figure 14: Comparison of growth rates for the long undulator and the segmented undulator.

IV. Conclusion

In this report we benchmarked two widely used FEL programs TDA3D and GENESIS. Good agreement exists between the theory and the TDA3D simulation results for the circular beam case. These have been reported here and elsewhere. Another benchmark performed here for TDA3D assures us that the version we are using is a good working version. The benchmark performed for GENESIS, which is a new program, indicates that the program is fast, accurate and reliable in treating general 3-D FEL interactions.

Acknowledgment

The formal effort of benchmark was initiated by S. Milton, who formed a group including S. Biedron, H. Freund, R. Dejus, Y.-C. Chae as the simulators of various codes. The result is presented in reference [9]. We appreciate all the discussions among collaborators. We acknowledge the numerous helps from S. Reich on GENESIS. Both TDA3D and GENESIS were obtained from S. Reiche and B. Faatz at DESY.

References

[1] T.M. Tran and J.S. Wurtele, "TDA-A THREE-DIMENSIONAL AXISYMMETRIC CODE FOR FREE-ELECTRON-LASER (FEL) SIMULATION," Computer Physics Communication 54 (1989) 263-272.

[2] T.M. Tran and J.S. Wurtele, "FREE-ELECTRON LASER SIMULATION TECHNIQUES," Physics Reports 195, No. 1 (1990) 1-21.

[3] S. Reiche and B. Faatz, "Upgrade of the Simulation Code TDA3D," will be published in NIM Proc. 20th Inter. FEL Conf, Williamsburg, VA, USA, 1998.

[4] S. Reiche, "GENESIS 1.3 - A Fully 3D Time Dependent FEL Simulation Code," will be published in NIM Proc. 20th Inter. FEL Conf., Williamsburg, VA, USA, 1998.

[5] L.H. Yu, S. Krinsky, R.L. Gluckstern, "Calculation of Universal Scaling Function for Free-Electron-Laser Gain," PRL Vol. 64, Number 25 (1990) 3011-3014.

[6] Y.H. Chin, K.-J. Kim, M. Xie, "Calculation of 3-D free electron laser gain: comparison with simulation and generalization to elliptical cross section," NIM A331 (1993) 429-436.

[7] M. Xie, "Design Optimization for an X-Ray Free Electron Laser Driven by SLAC LINAC," Proc. Of 1995 Part. Accel. Conf (1996) 183-185.

[8] K.-J. Kim, "Temporal and transverse Coherence of Self-Amplified Spontaneous Emission," in *TOWARDS X-RAY FREE ELECTRON LASERS*, AIP Conf. Proc. 413 (1997) 3-13.

[9] S.Biedron, et. el., “THE APS SASE FEL: MODELING AND CODE COMPARISON,” presented at 1999 Part. Accel. Conf., New York, NY, USA, 1999.